Role of Atmospheric Indices in Describing Shoreline Variability Along the Atlantic Coast of Europe

Gerd Masselink[1] , Bruno Castelle[2] , Tim Scott[1] , and Aikaterini Konstantinou[1]

[1]Coastal Processes Research Group, University of Plymouth, Plymouth, UK, [2]University Bordeaux, CNRS, Bordeaux INP, EPOC UMR, Pessac, France

Abstract Beaches are highly variable environments and respond to changes in wave forcing, themselves modulated by climate variability. Here, we analyze three high-quality beach profile data sets to robustly investigate, for the first time, the link between shoreline change, wave forcing and climate variability along the Atlantic coast of Europe. Winter wave conditions are strongly associated with North Atlantic Oscillation (NAO) and Western Europe Pressure Anomaly (WEPA), with WEPA explaining 50%–80% of the winter wave power variability. Shoreline variability during winter is also strongly linked to NAO and WEPA, with WEPA explaining 25% of the winter shoreline variability. Winter wave conditions and associated shoreline variability are both unrelated to El Nino Southern Oscillation. In addition to the atmospherically-forced beach morphological response, shoreline change also depends strongly on the antecedent morphology as evidenced by significant correlations between summer/winter shoreline response and the shoreline position at the start of each season.

Plain Language Summary Beaches change as a result of changes in the wave conditions, and the weather and climate controls wave conditions. We surveyed two beaches in SW England and one beach in SW France every month for more than 15 years and analyzed these data to look, for the first time, at the connections between beach change, waves and climate along the Atlantic coast of Europe. Atmospheric indices are numbers that tell us about large-scale weather, and the North Atlantic Oscillation and the Western Europe Pressure Anomaly (WEPA) are powerful indices that describe the weather in the north-east Atlantic. We found that especially WEPA is strongly correlated with winter waves and beach change during the winter months for all three study sites. We also found that beach change over the summer and winter season depends very much on whether the beach is relatively healthy or depleted of sediment.

1. Introduction

Shorelines are temporally highly variable and amongst the different timescales of shoreline change, the interannual and decadal timescales are of particular interest to coastal scientists as they reflect the integrated system response to the Earth's climate and its natural modes of variability. On these short-to-medium time scales, wave variability is the main driver for shoreline change and beaches respond to individual storms (Harley et al., 2017), storm clusters (Dissanayake et al., 2015), seasonal variation in wave conditions (Masselink & Pattiaratchi, 2001) and inter-annual to decadal changes in wave forcing (Castelle et al., 2018). Shorelines are also expected to change over long-term (>25 years) time scales, for example, due to sea-level rise, but it has been challenging to identify and isolate the modest and longer-term shoreline trends from the much more dynamic and short-to-medium term changes imposed by wave climate variability (Ghanavati et al., 2023). Both wave-driven cross-shore and longshore sediment transport processes are responsible for changes in beach morphology and shoreline position, with cross-shore processes generally dominating seasonal and annual coastal change, whereas longshore processes tend to dominate the coastal response over decadal times (Vitousek et al., 2017).

Temporal changes in wave forcing are controlled by large-scale weather patterns and their variability. Across the Pacific Ocean basin, the El Niño-Southern Oscillation (ENSO) is the dominant mode of interannual climate variability and is closely associated with wave conditions (Boucharel et al., 2021). In the Indian Ocean, seasonal extreme wave heights are associated with different phase combinations of ENSO and the Indian Ocean Dipole IOD (Kumar et al., 2019). In the north Atlantic, the North Atlantic Oscillation (NAO) is the dominant mode of atmospheric variability and is strongly associated with wave conditions, whereby positive phases of NAO are associated with increased winter wave conditions across the northeast Atlantic (Dodet et al., 2010), including for

Scotland (Commin et al., 2017) and Norway (Feng et al., 2014). On the other hand, negative phases of NAO are associated with energetic wave conditions along the south coast of Spain (Plomaritis et al., 2015). These dominant atmospheric circulation patterns can be quantified using indices, generally based on a measure of spatial variability in sea surface temperature or atmospheric pressure, and can be correlated with wave parameters.

For the northeast Atlantic, Castelle et al. (2017a) recently introduced a new atmospheric index, the Western Europe Pressure Anomaly (WEPA), based on the sea level pressure (SLP) gradient between the Valentia (Ireland) and Santa Cruz de Tenerife (Canary Islands). The WEPA positive phase reflects an intensified and southward-shifted SLP difference between the Icelandic low and the Azores high, driving severe storms that funnel high-energy waves toward western Europe southward of 52°N. The WEPA index was found to show a very strong correlation with winter wave conditions for the entire Atlantic European seaboard, from Ireland (52°N) to Spain (42°N), significantly outperforming NAO as a winter wave height predictor. Within the UK and Ireland, Scott et al. (2021) used wave model data from 63 locations and found that winter-averaged expressions of six leading atmospheric indices (including NAO and WEPA) were strongly correlated with both total and directional winter wave power. Notably, the predictive power of the climate indices displayed a strong geographical dependency, with NAO, and especially WEPA, being the most successful predictor for Atlantic storm waves. More regionally, Wiggins et al. (2020) investigated the characteristics of the strong bidirectional wave climate along the SE of England. They showed south-westerly wave power was well correlated to WEPA > 0, whilst easterly wave power was well correlated with NAO < 0.

Since wave height variability is strongly linked to coastal dynamics, it can therefore be hypothesized that atmospheric indices are also linked to coastal change. Almar et al. (2023) used this hypothesis on a global scale by developing a conceptual global model based on satellite-derived shoreline (SDS) positions from 1993 to 2019 and a variety of reanalysis products. They argue that global interannual shoreline changes are largely driven by different ENSO regimes and their complex inter-basin teleconnections, but reported correlations for the NE Atlantic appear weak. Nevertheless, extreme coastal erosion along the west coast of the US is unequivocally associated with strong El Niño events (Barnard et al., 2011, 2017; Young et al., 2018). Recently, Vos et al. (2023) used 38 years of Landsat imagery to map shoreline variability around the Pacific Rim and identified coherent, albeit regionally varying, patterns of beach erosion and accretion controlled by ENSO.

Similar efforts have been made to find associations between atmospheric indices and coastal change for the Atlantic coast of Europe. Masselink et al. (2014) suggested, based on analysis of a decade of video monitoring data from a sandy beach in SW England, that beach state and bar morphology is related to NAO. Wiggins et al. (2020) analyzed a decade of beach monitoring data from gravel beaches in SW England and found that beach rotation was related to WEPA for some beaches. Additionally, the 2013/2014 winter, which was the most energetic winter on record in terms of wave conditions and caused unprecedented beach erosion along the entire Atlantic coast of Europe (Masselink et al., 2016a), was characterized by the highest winter WEPA value since 1948. Finally, Castelle et al. (2022) investigated the 1984–2020 time- and space-evolution of 269 km of high-energy meso-macrotidal sandy coast in SW France using SDS data and found that the interannual shoreline variability was strongly correlated with the winter WEPA, outscoring other conventional teleconnection pattern indices (e.g., NAO). The attraction of identifying causal links between atmospheric indices and shoreline change is that it may facilitate modeling future shoreline dynamics without the need for wave modeling (Robinet et al., 2016), for example, to obtain season-ahead forecast of coastal change (Scott et al., 2021).

This paper builds on previous work along the Atlantic coast of Europe and uses a 17-year data set of monthly survey data collected at two beaches in SW England, Perranporth (sand) and Slapton Sands (gravel), and a 20-year high-frequency data set of from sandy beach in SW France (Truc Vert) to investigate the link between atmospheric indices, wave conditions and shoreline change. This is a first attempt at a wider scale (NW Atlantic coast) assessment of the links between climate patterns and shoreline change and this work represents a crucial step needed to gain confidence before investigating climate-shoreline links in larger-scale SDS-based studies.

2. Results

2.1. Perranporth

Throughout the paper, winter and summer refers to the periods December–March and April–November, respectively. Winter wave power ΣP at Perranporth (Figure 1a) is positively correlated with winter NAO (Figure 1c;
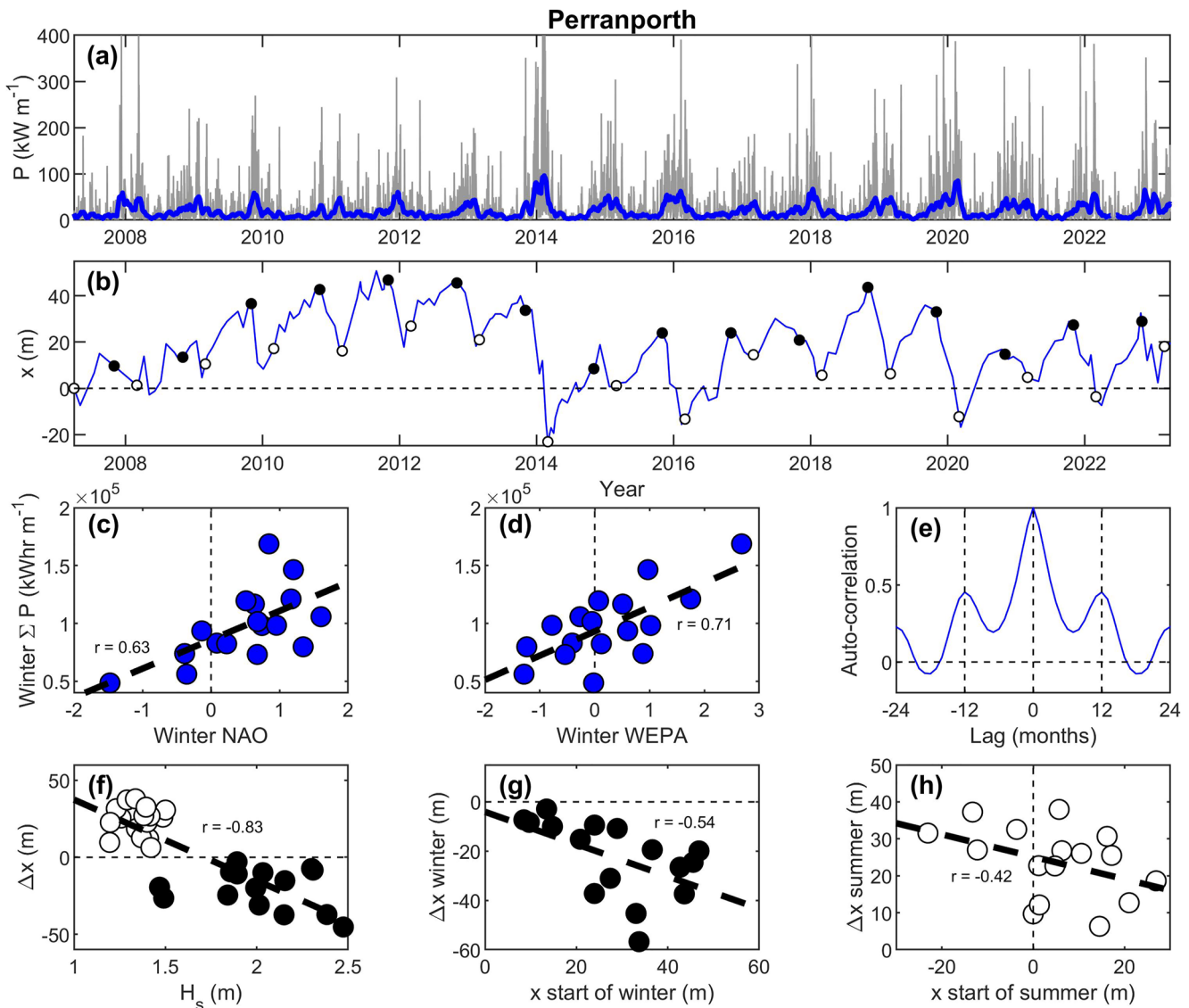
Figure 1. Wave conditions and shoreline response for Perranporth: (a) time series of wave power P (gray line) and 30-day moving average of the wave power (blue line); (b) time series of monthly shoreline position x (0 m ODN) relative to start of the survey period with start of winter (1 December) and summer (1 April) marked by black and white circles, respectively; (c,d) scatter plot of winter wave power ΣP versus winter NAO and WEPA; (e) auto-correlation function of the monthly survey data; (f) shoreline change Δx versus season-averaged significant wave height H_s with black and white circles representing winter and summer, respectively; (g) Δx over winter season versus x at the start of winter; and (h) Δx over summer season versus x at the start of summer. Dashed lines in (c), (e), (f), and (g) represent lines of best fit with Pearson r indicated in the plots.

$r = 0.63$, $p = 0.01$) and WEPA (Figure 1d; $r = 0.71$, $p = 0.00$), indicating that positive phases of both atmospheric indices are associated with enhanced storminess. No significant correlation was found with ENSO ($r = -0.23$; $p = 0.36$). The monthly time series of shoreline position x at Perranporth shows a strong seasonal variation with an amplitude of 20–30 m (Figure 1b). No long-term trend is apparent, but a dominant feature of the time series is a shoreline retreat of c. 60 m during the 2013/2014 winter. All summers are characterized by shoreline progradation ($\Delta x > 0$) and all winters resulted in shoreline retreat ($\Delta x < 0$). The seasonality in shoreline change is further demonstrated by the auto-correlation function of the monthly survey data, which shows a distinct secondary peak at 12 months (Figure 1e). Beach morphological change at Perranporth is forced by variations in the wave conditions, but is also influenced by the antecedent morphology. A strong correlation between the seasonal shoreline change Δx and the seasonally averaged wave height H_s is apparent (Figure 1f; $r = -0.83$, $p = 0.00$)), with $H_s = 1.5$ m broadly separating shoreline advance and retreat. Seasonal shoreline response is also affected by the shoreline position at the start of the season: winter erosion ($\Delta x < 0$) is encouraged when the beach is relatively
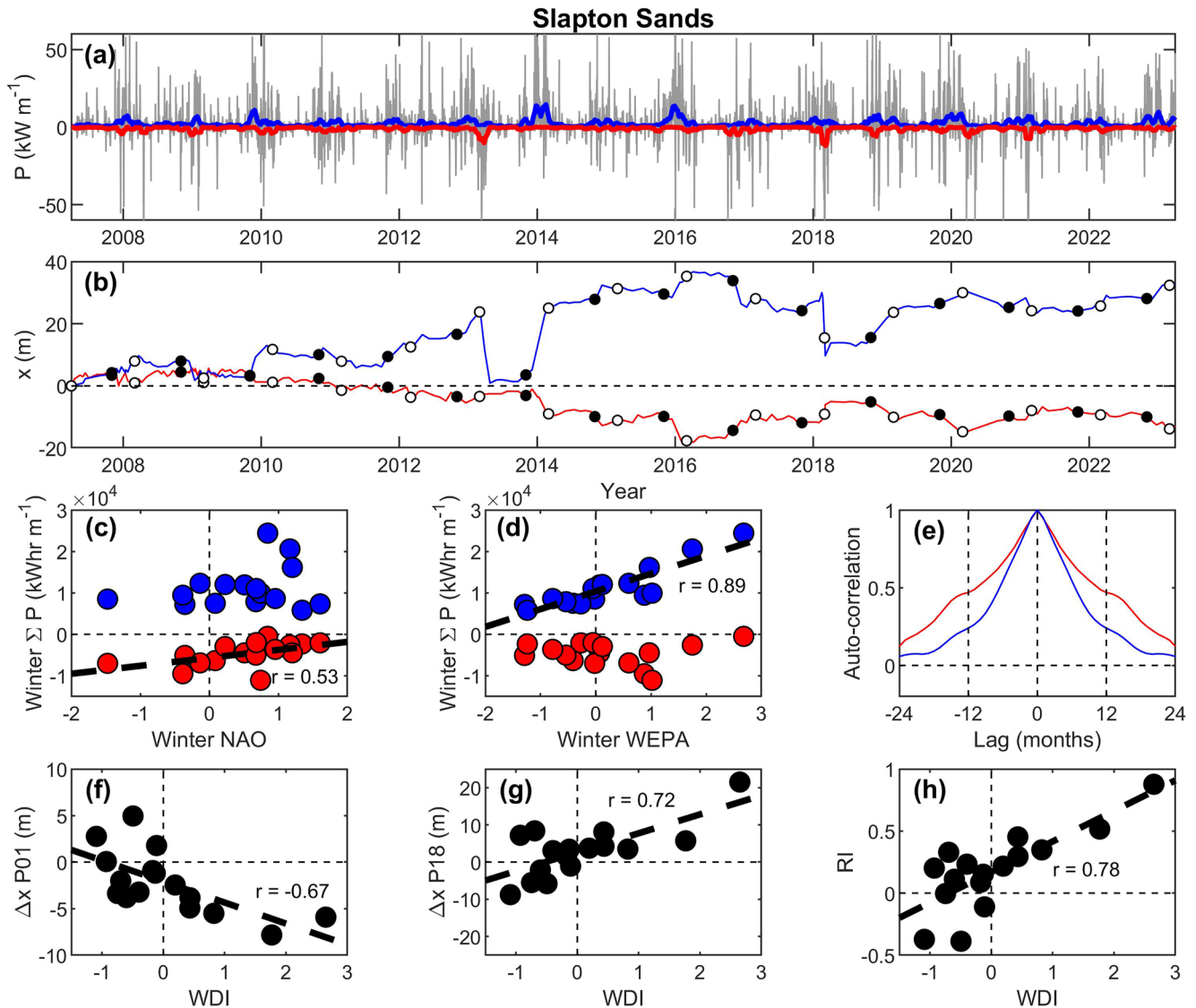
Figure 2. Wave conditions and shoreline response for Slapton Sands: (a) time series of wave power P (gray line) and 30-day moving average of the southerly (>135°; blue line) and easterly (<135°; red line) wave power; (b) time series of monthly shoreline position x (0 m ODN) for P01 (red) and P18 (blue) relative to start of the survey period with start of winter (1 December) and summer (1 April) marked by black and white circles, respectively; (c, d) scatter plot of winter wave power from the south ΣP_{south} (blue) and the east ΣP_{east} (red) versus winter NAO and WEPA; (e) auto-correlation function of the monthly survey data for P01 (red line) and P18 (blue line); (h, i) winter shoreline change Δx at P01 and P18 versus Wave power Directionality Index WDI; and (j) Rotation Index RI versus WDI. Positive and negative values for WDI represent above-average contribution of southerly and easterly wave power, respectively, and positive and negative values for RI represent clockwise and anti-clockwise beach rotation, respectively. Dashed lines in (c), (d), (f), (g), and (h) represent lines of best fit with Pearson r indicated in the plots.

wide at the start of the winter (Figure 1g; $r = -0.54$, $p = 0.03$), while summer accretion is promoted by a relatively depleted beach at the start of summer (Figure 1h; $r = -0.42$, $p = 0.10$).

2.2. Slapton Sands

The wave climate at Slapton Sands is bi-directional with 70% of the winter wave power generated by southerly swell waves from the Atlantic and 30% by easterly wind waves generated across the Channel (Figure 2a). Southerly wave power from the Atlantic ΣP_{south} is positively correlated with winter WEPA (Figure 2d; $r = 0.89$, $p = 0.00$), whereas easterly wave power ΣP_{east}, is correlated with winter NAO (Figure 2c; $r = 0.53$, $p = 0.03$) indicating that large ΣP_{east} values are associated with negative NAO). No significant correlations were found with ENSO (with ΣP_{south}: $r = -0.1$, $p = 0.70$; with ΣP_{east}: $r = -0.34$, $p = 0.20$). Shoreline changes at Slapton

Sands are characterized by an antiphase relationship between the south and north end of the beach (P01 and P18, respectively) (Figure 2b), representing a rotational response. Over the whole survey period, the southern profile shows a shoreline retreat of 15 m, whereas the northern profile displays a shoreline advance of 30 m. Seasonal shoreline variation is not obvious, but the largest shoreline changes are generally associated with winter waves. Both winter waves and summer waves can result in a shoreline advance, as well as retreat. The lack of seasonality is further demonstrated by the absence of a 12-month peak in the auto-correlation function of the monthly survey data for both transects (Figure 2e).

The more complex beach volume changes at Slapton Sands, involving longshore redistribution of sediment, require consideration of the directional wave energy fluxes for the opposing ends of the beach. Large values of the seasonally integrated southerly wave power ΣP_{south} are associated with shoreline retreat ($\Delta x < 0$) and advance ($\Delta x > 0$) for P01 and P18, respectively (Figures S8a and S8c in Supporting Information S1), and a clockwise beach rotation. The beach response to the seasonally integrated easterly wave power ΣP_{east} is not obvious (Figures S8b and S8d in Supporting Information S1). A better way to parameterize the bi-directional wave conditions at Slapton Sands is through the Wave power Directionality Index WDI (see Methods section in Supporting Information S1), which quantifies the seasonal balance between the two directional wave components compared to the long-term average balance. WDI is significantly correlated with Δx at P01 (Figure 2f; $r = -0.67$, $p = 0.00$) and at P18 (Figure 2g; $r = 0.72$, $p = 0.00$). By combining the shoreline responses at the opposing ends of Slapton Sands in the Rotation Index RI (see Methods section in Supporting Information S1) and relating this to WDI provides an even better explanation of the rotational beach response (Figure 2h; $r = -0.78$, $p = 0.00$): for WDI > 0, southerly waves are more common than average and/or easterly waves are less common than average, and the beach at P01 and P18 retreats and advances, respectively, and the reverse is true for WDI < 0. So, clockwise (RI > 0) and anti-clockwise (RI < 0) rotation are associated with WDI > 0 and WDI < 0, respectively.
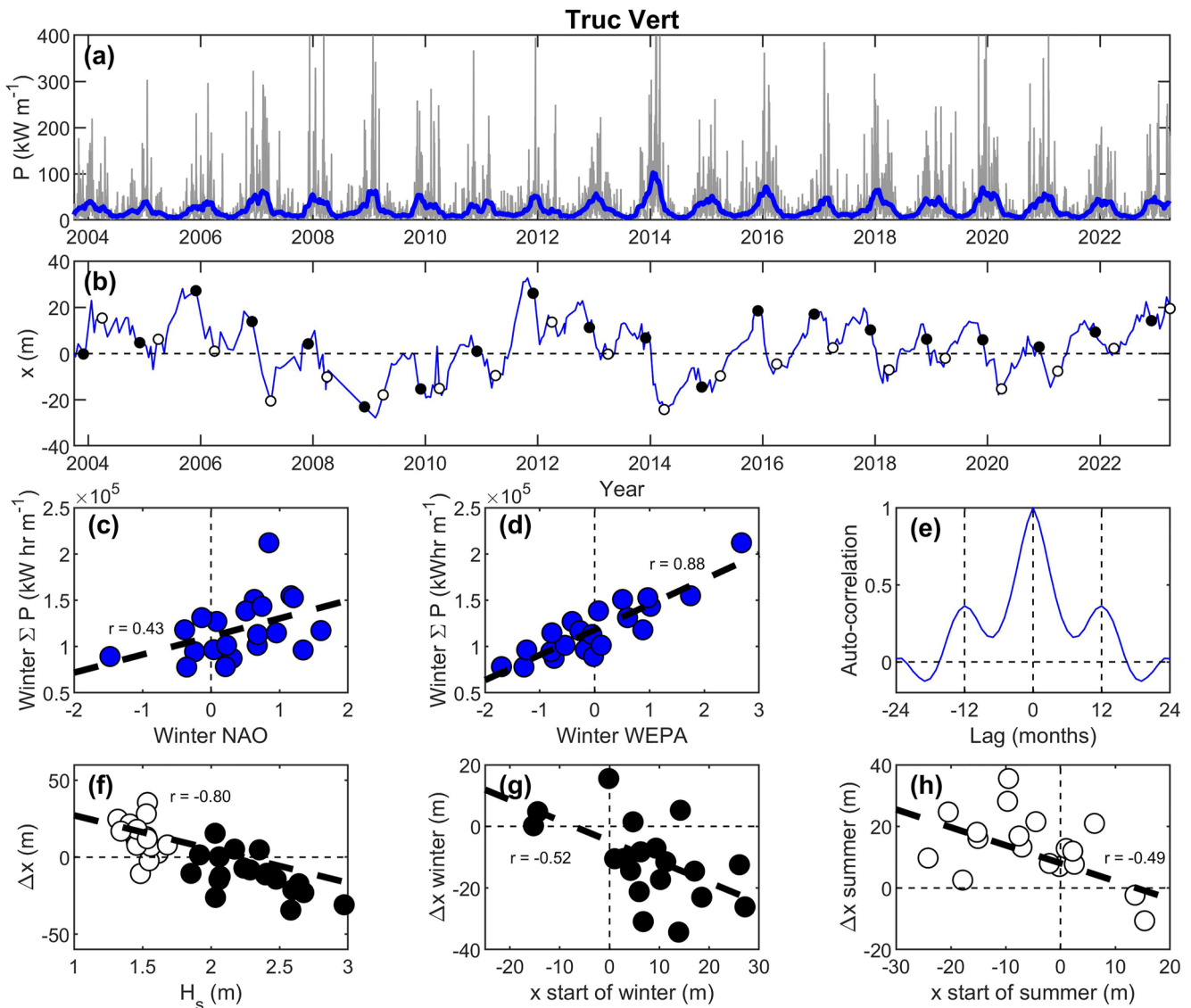
2.3. Truc Vert

The relationship between atmospheric indices, wave forcing and shoreline dynamics at Truc Vert is very similar to that at Perranporth, despite the more energetic waves and smaller tides. Winter wave power ΣP is positively correlated with winter NAO (Figure 3c; $r = 0.43$, $p = 0.05$) and WEPA (Figure 3d; $r = 0.88$, $p = 0.00$), and no significant correlation was found with ENSO ($r = -0.09$, $p = 0.71$). The shoreline at Truc Vert shows no long-term trend, but has a strong seasonal variation with an amplitude of 10–20 m (Figure 3b) and the auto-correlation function of the monthly survey data shows a distinct secondary peak at 12 months (Figure 3e). The 2013/2014 winter caused the largest shoreline retreat, and it is further noted that five of the 20 winters were characterized by shoreline progradation and that shoreline retreat occurred over three of the 19 summers. In common with Perranporth, beach morphological change on Truc Vert is also influenced by antecedent morphology. A strong correlation between the seasonal shoreline change Δx and the seasonally averaged wave height H_s is apparent (Figure 3f; $r = -0.80$, $p = 0.00$), but the H_s value separating shoreline advance and retreat is not very distinct. Winter erosion ($\Delta x < 0$) is encouraged when the beach is relatively wide at the start of the winter (Figure 3g; $r = -0.52$, $p = 0.02$), while summer accretion is promoted by a relatively depleted beach at the start of summer (Figure 3h; $r = -0.49$, $p = 0.04$). The shoreline response on Truc Vert is more complex than at Perranporth and this is likely related to the more energetic conditions at the former site over the summer period (April–November).

2.4. Role of Atmospheric Indices

The relationship between shoreline change Δx and atmospheric indices for the winter season is explored in Figure 4. The strength of the correlations between climate indices and wave forcing and shoreline response (Pearson r and associated p-values) are listed in Table S2 in Supporting Information S1.

The winter wave forcing conditions ($\Sigma P - \langle\Sigma P\rangle$ for Perranporth and Truc Vert, and WDI for Slapton Sands) are plotted in a NAO-WEPA parameter space in Figures 4a, 4e, and 4c, respectively (no significant correlations were found with ENSO). The NAO+/WEPA+ quadrant is associated with the most energetic winter wave conditions at Perranporth and Truc Vert, and the largest positive WDI values for Slapton Sands. Both results are attributed to more energetic and/or frequent Atlantic storms under such climatic conditions (Castelle et al., 2017a). The other NAO/WEPA quadrants are characterized by more benign and below-average winter wave conditions for Perranporth and Truc Vert, and smaller positive or even negative WDI values for Slapton Sands. As WDI represents the

Figure 3. Wave conditions and shoreline response for Truc Vert (for caption, cf. Figure 1).

balance between southerly and easterly wave power, negative WDI values could be due to less energetic Atlantic wave conditions and/or more frequent easterly storm wave activity.

The winter beach response (Δx for Perranporth and Truc Vert, and RI for Slapton Sands) are also plotted in the NAO-WEPA parameter space (again, no significant correlations were found with ENSO). The most extensive winter shoreline retreat on Perranporth and Truc Vert is associated with the NAO+/WEPA+ quadrant (Figures 4b and 4f) and, of the two atmospheric indices, WEPA shows stronger correlations with Δx than NAO (Table S2 in Supporting Information S1). At Perranporth, all winters result in shoreline retreat (Figure 4b), but the calmest winters at Truc Vert are associated with shoreline advance (blue symbols in Figure 4f). For Slapton Sands, the NAO+/WEPA+ quadrant is characterized by the most pronounced clockwise rotation, quantified by RI, and the two winters with the largest RI values (2013/14 and 2015/16), plot at the top of the NAO+/WEPA+ quadrant (Figure 3d). Of the two climate indices, WEPA shows stronger correlation with RI than NAO (Table S2 in Supporting Information S1).

3. Discussion and Conclusions

The findings of this study confirm and expand previous studies on these three beaches (Castelle et al., 2020; McCarroll et al., 2023). Winter wave conditions for all sites are strongly associated with Atlantic climate indices
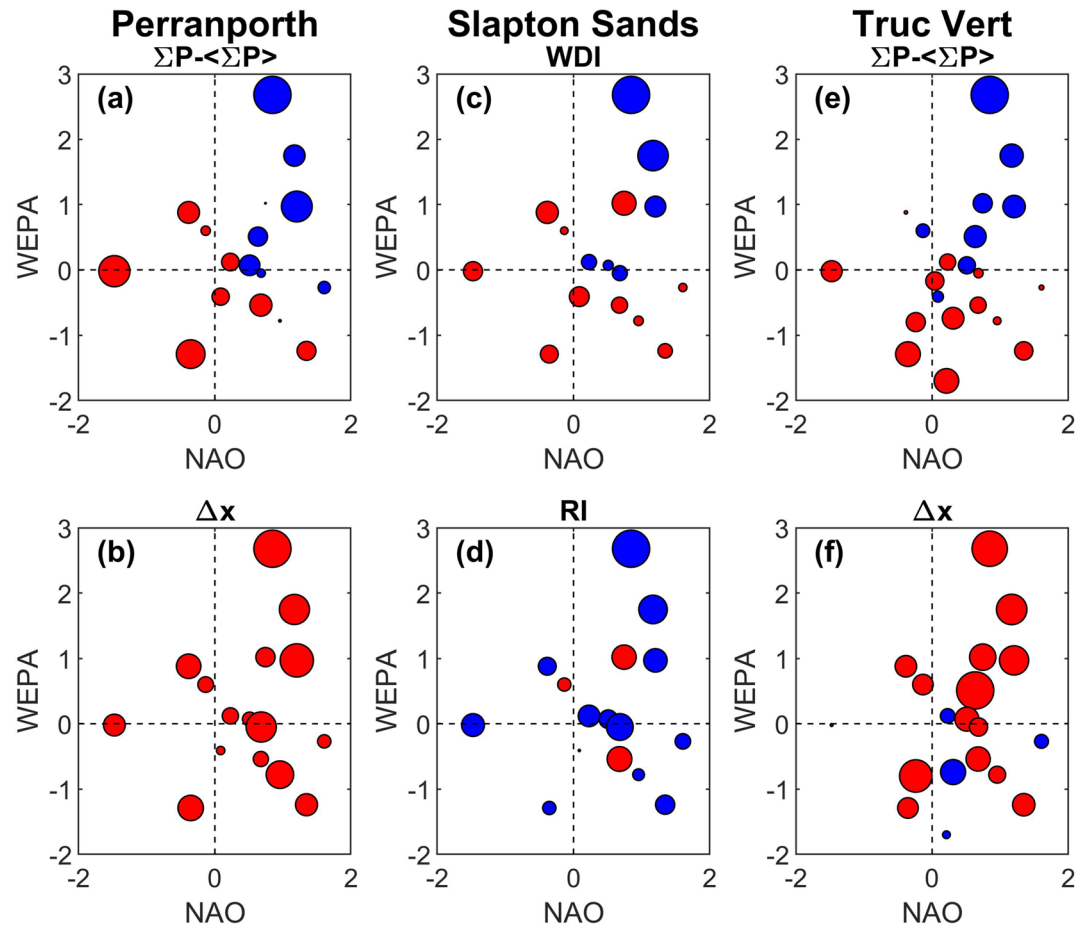
Figure 4. Wave and morphological response parameters representing the winter season plotted in NAO-WEPA parameter space: (a) winter wave power ΣP minus winter-averaged wave power $<\Sigma P>$ for Perranporth; (b) shoreline change Δx for Perranporth; (c) Wave power Directionality Index WDI for Slapton Sands; (d) Rotation Index RI for Slapton Sands; (e) winter wave power ΣP minus winter-averaged wave power $<\Sigma P>$ for Truc Vert; and (f) shoreline change Δx for Truc Vert. The size of the symbols is scaled by the absolute value of the plotted parameters, and red and blue symbols represent negative and positive values, respectively.

NAO and WEPA, and are unrelated to ENSO. Perranporth and Truc Vert, which are representative of exposed Atlantic sandy beaches, experience a unidirectional and strongly seasonal wave climate, driving a dominantly cross-shore and seasonal beach signal. Slapton Sands, which is a representative gravel beach on the south coast of England, experiences a bidirectional wave climate, driving a dominantly rotational beach response caused by a longshore redistribution of sediment. The morphodynamics on all beaches are strongly linked to Atlantic climate indices NAO and WEPA, and unrelated to ENSO. In addition to the strongly forced response, beach response on the exposed beaches (Perranporth and Truc Vert) also depends strongly on the beach state/volume at the start of each season.

The strongest statistically significant (at $p < 0.05$) correlations are found between WEPA and winter shoreline change; however, winter WEPA only explains c. 25% of the shoreline variability. There are other factors that are also important in driving shoreline change. First, shoreline response is not necessarily the result of sustained storm wave activity related to an exceptional atmospheric condition parameterized by an extreme value for a climate index (e.g., the 2013/2014 winter), and can be the result of a single event in an otherwise unremarkable winter. For example, the pronounced anti-clockwise rotation that occurred in the 2018/2019 winter on Slapton Sands (Figure 2) was the result of a single easterly storm (McCarroll et al., 2019) that occurred in a winter characterized by a positive NAO of 0.74. Second, shoreline dynamics on the exposed and cross-shore dominated beaches of Perranporth and Truc Vert showed relatively muted storm responses on beaches depleted due to previous energetic conditions, strongly suggesting the importance of antecedent conditions and beach

morphology, and an equilibrium-type beach response (Davidson, 2021; Splinter et al., 2014; Yates et al., 2009). The shoreline response of Slapton Sands appears also to be associated with disequilibrium, but operating over a decadal time scale. Over the 2004–2023 survey period, the shoreline at Slapton Sands exhibited a considerable clock-wise rotation and this has been suggested to be related to a multi-decadal trend in the balance between southerly and easterly wave power (Wiggins et al., 2017). Finally, the role of water levels during storm conditions should be considered as storm impacts are maximized if peak wave conditions coincide with extreme water levels (Masselink et al., 2016b; Young et al., 2018). As the Atlantic coast of Europe is not a surge-dominated coast, coincidence of peak storm and extreme water level is due to chance (Haigh et al., 2016), and not related to atmospheric indices.

The position of the intertidal shoreline was selected as the key coastal state indicator (CSI) for characterizing beach morphological response and was found to be highly correlated with the intertidal beach volume (Figure S4 in Supporting Information S1). The attraction of a shoreline-based CSI is obvious as it can be derived through remote sensing (aerial photography, video, satellites). Nevertheless, changes in the intertidal shoreline position are not necessarily representative of changes in the nearshore sediment budget if the subtidal region is considered as well (Harley et al., 2022). In addition, different shoreline contours respond at different dominant time scales (Montaño et al., 2021), for example, compared to the MSL contour, the dune foot responds in a less seasonal and more multi-annual fashion with significant set-back only occurring during a handful of winters (Burvingt & Castelle, 2023; Castelle et al., 2017b; Flor-Blanco et al., 2021; Masselink et al., 2022).

Winter values for climate indices (December–March) are generally used because they tend to have the strongest relation to wave climate and it is the climate hazards during winter (e.g., dune erosion, coastal flooding, overtopping) that are usually of most interest. So, here we demonstrate that shoreline response during winter is significantly correlated to winter WEPA, and, for example, Jalón-Rojas and Castelle (2021) show that precipitation and river flows over the winter period across most of Europe are also positively correlated with winter WEPA. From a coastal management point of view, it is of interest to determine the longevity of the winter storm impacts; therefore, the annual shoreline response (December–March) was correlated with winter WEPA (December–March) for Perranporth and Truc Vert. Compared to correlating winter WEPA with the winter shoreline response, Pearson r dropped from -0.54 ($p = 0.03$) to -0.40 ($p = 0.14$) for Perranporth, and from -0.52 ($p = 0.02$) to -0.46 ($p = 0.06$) for Truc Vert. The reduction in explanatory power of WEPA is due to the significant beach recovery that takes place over subsequent summers (Burvingt et al., 2018; Dodet et al., 2019; Konstantinou et al., 2021). Shoreline advance during summer is particularly pronounced after an extreme winter (Figures 1h and 3h).

Global studies of shoreline change based on satellite-derived shorelines (SDS) are becoming increasingly common (Almar et al., 2023; Ghanavati et al., 2023; Luijendijk et al., 2018; Mentaschi et al., 2018; Vousdoukas et al., 2020); however, concerns have been raised regarding satellite-derived global applications (Cooper et al., 2020; Zăinescu et al., 2023). To explore links between shoreline response and modes of climate variability, robust methodologies for deriving shorelines involving wave and/or tide corrections (Castelle et al., 2021; Vos et al., 2023) or time- and spatial-averaging techniques (Castelle et al., 2022; Warrick et al., 2023) must be applied. However, the typical time- and space-averaging windows and type of water-level correction are essentially site-specific (Konstantinou et al., 2023), which challenges such global application. Based on SDS, Almar et al. (2023) recently claimed that interannual shoreline changes at the global scale are largely driven by different ENSO regimes and their complex inter-basin teleconnections, including along the Atlantic coast of Europe. Noteworthy, the authors used uncorrected SDS data at 0.5° spaced transects. Critically, our contribution shows that, at three intensely monitored sites, which use conventional survey techniques from which accurate shoreline position can be derived, shoreline change is essentially uncorrelated with ENSO. This is perhaps not surprising, as there is no clear consensus as to whether a robust ENSO signal can be detected in the north Atlantic and West Europe region (Toniazzo & Scaife, 2006). We advocate that future, regional to global, SDS assessment must use carefully ground-truth validated, high-resolution data accounting for the diversity of coastal settings to provide robust conclusions on the link between climate modes of variability and coastal response.

Data Availability Statement

The data used in this study are freely available at University of Plymouth Pearl repository via Masselink et al. (2023).

References

Almar, R., Boucharel, J., Graffin, M., Abessolo, G. O., Thoumyre, G., Papa, F., et al. (2023). Influence of El Niño on the variability of global shoreline position. *Nature Communications*, *14*(1), 3133. https://doi.org/10.1038/s41467-023-38742-9

Barnard, P. L., Allan, J., Hansen, J. E., Kaminsky, G. M., Ruggiero, P., & Doria, A. (2011). The impact of the 2009–10 El Niño Modoki on U.S. West Coast beaches. *Geophysical Research Letters*, *38*(13), L13604. https://doi.org/10.1029/2011GL047707

Barnard, P. L., Hoover, D., Hubbard, D. M., Snyder, A., Ludka, B. C., Allan, J., et al. (2017). Extreme oceanographic forcing and coastal response due to the 2015–2016 El Niño. *Nature Communications*, *8*(1), 14365. https://doi.org/10.1038/ncomms14365

Boucharel, J., Almar, R., Kestenare, E., & Jin, F.-F. (2021). On the influence of ENSO complexity on Pan-Pacific coastal wave extremes. *Proceedings of the National Academy of Sciences*, *118*(47), e2115599118. https://doi.org/10.1073/pnas.2115599118

Burvingt, O., & Castelle, B. (2023). Storm response and multi-annual recovery of eight coastal dunes spread along the Atlantic coast of Europe. *Geomorphology*, *435*, 108735. https://doi.org/10.1016/j.geomorph.2023.108735

Burvingt, O., Masselink, G., Scott, T., Davidson, M., & Russell, P. (2018). Climate forcing of regionally-coherent extreme storm impact and recovery on embayed beaches. *Marine Geology*, *401*, 112–128. https://doi.org/10.1016/j.margeo.2018.04.004

Castelle, B., Bujan, S., Ferreira, S., & Dodet, G. (2017b). Foredune morphological changes and beach recovery from the extreme 2013/2014 winter at a high-energy sandy coast. *Marine Geology*, *385*, 41–55. https://doi.org/10.1016/j.margeo.2016.12.006

Castelle, B., Bujan, S., Marieu, V., & Ferreira, S. (2020). 16 years of topographic surveys of rip-channelled high-energy meso-macrotidal sandy beach. *Scientific Data*, *7*(1), 410. https://doi.org/10.1038/s41597-020-00750-5

Castelle, B., Dodet, G., Masselink, G., & Scott, T. (2017a). A new climate index controlling winter wave activity along the Atlantic coast of Europe: The West Europe pressure anomaly. *Geophysical Research Letters*, *44*(3), 1384–1392. https://doi.org/10.1002/2016GL072379

Castelle, B., Dodet, G., Masselink, G., & Scott, T. (2018). Increased winter-mean wave height, variability, and periodicity in the Northeast Atlantic over 1949–2017. *Geophysical Research Letters*, *45*(8), 3586–3596. https://doi.org/10.1002/2017gl076884

Castelle, B., Masselink, G., Scott, T., Stokes, C., Konstantinou, A., Marieu, V., & Bujan, S. (2021). Satellite-derived shoreline detection at a high-energy meso-macrotidal beach. *Geomorphology*, *383*, 107707. https://doi.org/10.1016/j.geomorph.2021.107707

Castelle, B., Ritz, A., Marieu, V., Nicolae Lerma, A., & Vandenhove, M. (2022). Primary drivers of multidecadal spatial and temporal patterns of shoreline change derived from optical satellite imagery. *Geomorphology*, *413*, 108360. https://doi.org/10.1016/j.geomorph.2022.108360

Commin, A. N., French, A. S., Marasco, M., Loxton, J., Gibb, S. W., & McClatchey, J. (2017). The influence of the North Atlantic Oscillation on diverse renewable generation in Scotland. *Applied Energy*, *205*, 855–867. https://doi.org/10.1016/j.apenergy.2017.08.126

Cooper, J. A. G., Masselink, G., Coco, G., Short, A. D., Castelle, B., Rogers, K., et al. (2020). Sandy beaches can survive sea-level rise. *Nature Climate Change*, *10*(11), 993–995. https://doi.org/10.1038/s41558-020-00934-2

Davidson, M. (2021). Forecasting coastal evolution on time-scales of days to decades. *Coastal Engineering*, *168*, 103928. https://doi.org/10.1016/j.coastaleng.2021.103928

Dissanayake, P., Brown, J., Wisse, P., & Karunarathna, H. (2015). Effects of storm clustering on beach/dune evolution. *Marine Geology*, *370*, 63–75. https://doi.org/10.1016/j.margeo.2015.10.010

Dodet, G., Bertin, X., & Taborda, R. (2010). Wave climate variability in the North-East Atlantic Ocean over the last six decades. *Ocean Modelling*, *31*(3), 120–131. https://doi.org/10.1016/j.ocemod.2009.10.010

Dodet, G., Castelle, B., Masselink, G., Scott, T., Davidson, M., Floc'H, F., et al. (2019). Beach recovery from extreme storm activity during the 2013-14 winter along the Atlantic coast of Europe. *Earth Surface Processes and Landforms*, *44*(1), 393–401. https://doi.org/10.1002/esp.4500

Feng, X., Tsimplis, M. N., Yelland, M. J., & Quartly, G. D. (2014). Changes in significant and maximum wave heights in the Norwegian Sea. *Global and Planetary Change*, *113*, 68–76. https://doi.org/10.1016/j.gloplacha.2013.12.010

Flor-Blanco, G., Alcántara-Carrió, J., Jackson, D. W. T., Flor, G., & Flores-Soriano, C. (2021). Coastal erosion in NW Spain: Recent patterns under extreme storm wave events. *Geomorphology*, *387*, 107767. https://doi.org/10.1016/j.geomorph.2021.107767

Ghanavati, M., Young, I., Kirezci, E., Ranasinghe, R., Duong, T. M., & Luijendijk, A. P. (2023). An assessment of whether long-term global changes in waves and storm surges have impacted global coastlines. *Scientific Reports*, *13*(1), 11549. https://doi.org/10.1038/s41598-023-38729-y

Haigh, I. D., Wadey, M. P., Wahl, T., Ozsoy, O., Nicholls, R. J., Brown, J. M., et al. (2016). Spatial and temporal analysis of extreme sea level and storm surge events around the coastline of the UK. *Scientific Data*, *3*(1), 160107. https://doi.org/10.1038/sdata.2016.107

Harley, M. D., Masselink, G., Ruiz de Alegría-Arzaburu, A., Valiente, N. G., & Scott, T. (2022). Single extreme storm sequence can offset decades of shoreline retreat projected to result from sea-level rise. *Communications Earth & Environment*, *3*(1), 112. https://doi.org/10.1038/s43247-022-00437-2

Harley, M. D., Turner, I. L., Kinsela, M. A., Middleton, J. H., Mumford, P. J., Splinter, K. D., et al. (2017). Extreme coastal erosion enhanced by anomalous extratropical storm wave direction. *Scientific Reports*, *7*(1), 6033. https://doi.org/10.1038/s41598-017-05792-1

Jalón-Rojas, I., & Castelle, B. (2021). Climate control of multidecadal variability in river discharge and precipitation in western Europe. *Water*, *13*(3), 257. https://doi.org/10.3390/w13030257

Konstantinou, A., Scott, T., Masselink, G., Stokes, K., Conley, D., & Castelle, B. (2023). Satellite-based shoreline detection along high-energy macrotidal coasts and influence of beach state. *Marine Geology*, *462*, 107082. https://doi.org/10.1016/j.margeo.2023.107082

Konstantinou, A., Stokes, C., Masselink, G., & Scott, T. (2021). The extreme 2013/14 winter storms: Regional patterns in multi-annual beach recovery. *Geomorphology*, *389*, 107828. https://doi.org/10.1016/j.geomorph.2021.107828

Kumar, P., Kaur, S., Weller, E., & Min, S.-K. (2019). Influence of natural climate variability on the extreme ocean surface wave heights over the Indian Ocean. *Journal of Geophysical Research: Oceans*, *124*(8), 6176–6199. https://doi.org/10.1029/2019JC015391

Luijendijk, A., Hagenaars, G., Ranasinghe, R., Baart, F., Donchyts, G., & Aarninkhof, S. (2018). The state of the world's beaches. *Scientific Reports*, *8*(1), 1–11. https://doi.org/10.1038/s41598-018-24630-6

Masselink, G., Austin, M., Scott, T., Poate, T., & Russell, P. (2014). Role of wave forcing, storms and NAO in outer bar dynamics on a high-energy, macro-tidal beach. *Geomorphology*, *226*, 76–93. https://doi.org/10.1016/j.geomorph.2014.07.025

Masselink, G., Brooks, S., Poate, T., Stokes, C., & Scott, T. (2022). Coastal dune dynamics in embayed settings with sea-level rise – Examples from the exposed and macrotidal north coast of SW England. *Marine Geology*, *450*, 106853. https://doi.org/10.1016/j.margeo.2022.106853

Masselink, G., Castelle, B., Scott, T., Dodet, G., Suanez, S., Jackson, D., & Floc'h, F. (2016b). Extreme wave activity during 2013/2014 winter and morphological impacts along the Atlantic coast of Europe. *Geophysical Research Letters*, *43*(5), 2135–2143. https://doi.org/10.1002/2015gl067492

Masselink, G., Castelle, B., Scott, T., & Konstantinou, A. (2023). Role of atmospheric indices in describing shoreline variability along the Atlantic coast of Europe [Dataset]. University of Plymouth PEARL Repository. https://pearl.plymouth.ac.uk/handle/10026.1/21246

Masselink, G., & Pattiaratchi, C. (2001). Seasonal changes in beach morphology along the sheltered coastline of Perth, Western Australia. *Marine Geology*, *172*(3–4), 243–263. https://doi.org/10.1016/S0025-3227(00)00128-6

Masselink, G., Scott, T., Poate, T., Russell, P., Davidson, M., & Conley, D. (2016a). The extreme 2013/2014 winter storms: Hydrodynamic forcing and coastal response along the southwest coast of England. *Earth Surface Processes and Landforms*, *41*(3), 378–391. https://doi.org/10.1002/esp.3836

McCarroll, R. J., Masselink, G., Wiggins, M., Scott, T., Billson, O., Conley, D. C., & Valiente, N. G. (2019). High-efficiency gravel longshore sediment transport and headland bypassing over an extreme wave event. *Earth Surface Processes and Landforms*, *44*(13), 2720–2727. https://doi.org/10.1002/esp.4692

McCarroll, R. J., Valiente, N. G., Wiggins, M. H., Scott, T., & Masselink, G. (2023). Coastal survey data for Perranporth beach and start Bay in southwest England (2006–2021). Scientific data (Vol. *10*).

Mentaschi, L., Vousdoukas, M. I., Pekel, J.-F., Voukouvalas, E., & Feyen, L. (2018). Global long-term observations of coastal erosion and accretion. *Scientific Reports*, *8*(1), 12876. https://doi.org/10.1038/s41598-018-30904-w

Montaño, J., Coco, G., Chataigner, T., Yates, M., Le Dantec, N., Suanez, S., et al. (2021). Time-scales of a dune-beach system and implications for shoreline modeling. *Journal of Geophysical Research: Earth Surface*, *126*(11), e2021JF006169. https://doi.org/10.1029/2021JF006169

Plomaritis, T. A., Benavente, J., Laiz, I., & Del Río, L. (2015). Variability in storm climate along the Gulf of Cadiz: The role of large scale atmospheric forcing and implications to coastal hazards. *Climate Dynamics*, *45*(9), 2499–2514. https://doi.org/10.1007/s00382-015-2486-4

Robinet, A., Castelle, B., Idier, D., Le Cozannet, G., Déqué, M., & Charles, E. (2016). Statistical modeling of interannual shoreline change driven by North Atlantic climate variability spanning 2000–2014 in the Bay of Biscay. *Geo-Marine Letters*, *36*(6), 479–490. https://doi.org/10.1007/s00367-016-0460-8

Scott, T., McCarroll, R. J., Masselink, G., Castelle, B., Dodet, G., Saulter, A., et al. (2021). Role of atmospheric indices in describing inshore directional wave climate in the United Kingdom and Ireland. *Earth's Future*, *9*(5), e2020EF001625. https://doi.org/10.1029/2020EF001625

Splinter, K. D., Turner, I. L., Davidson, M. A., Barnard, P., Castelle, B., & Oltman-Shay, J. (2014). A generalized equilibrium model for predicting daily to interannual shoreline response. *Journal of Geophysical Research: Earth Surface*, *119*(9), 1936–1958. https://doi.org/10.1002/2014JF003106

Toniazzo, T., & Scaife, A. A. (2006). The influence of ENSO on winter North Atlantic climate. *Geophysical Research Letters*, *33*(24), L24704. https://doi.org/10.1029/2006GL027881

Vitousek, S., Barnard, P. L., Limber, P., Erikson, L., & Cole, B. (2017). A model integrating longshore and cross-shore processes for predicting long-term shoreline response to climate change. *Journal of Geophysical Research: Earth Surface*, *122*(4), 782–806. https://doi.org/10.1002/2016JF004065

Vos, K., Harley, M. D., Turner, I. L., & Splinter, K. D. (2023). Pacific shoreline erosion and accretion patterns controlled by El Niño/Southern Oscillation. *Nature Geoscience*, *16*(2), 140–146. https://doi.org/10.1038/s41561-022-01117-8

Vousdoukas, M. I., Ranasinghe, R., Mentaschi, L., Plomaritis, T. A., Athanasiou, P., Luijendijk, A., & Feyen, L. (2020). Sandy coastlines under threat of erosion. *Nature Climate Change*, *10*(3), 260–263. https://doi.org/10.1038/s41558-020-0697-0

Warrick, J. A., Vos, K., Buscombe, D., Ritchie, A. C., & Curtis, J. A. (2023). A large sediment accretion wave along a Northern California Littoral Cell. *Journal of Geophysical Research: Earth Surface*, *128*(7), e2023JF007135. https://doi.org/10.1029/2023JF007135

Wiggins, M., Scott, T., Masselink, G., McCarroll, R. J., & Russell, P. (2020). Predicting beach rotation using multiple atmospheric indices. *Marine Geology*, *426*, 106207. https://doi.org/10.1016/j.margeo.2020.106207

Wiggins, M., Scott, T., Masselink, G., Russell, P., Castelle, B., & Dodet, G. (2017). The role of multi-decadal climate variability in controlling coastal dynamics: Re-interpretation of the 'lost village of Hallsands'.

Yates, M. L., Guza, R. T., & O'Reilly, W. C. (2009). Equilibrium shoreline response: Observations and modeling. *Journal of Geophysical Research*, *114*(C9), C09014. https://doi.org/10.1029/2009JC005359

Young, A. P., Flick, R. E., Gallien, T. W., Giddings, S. N., Guza, R. T., Harvey, M., et al. (2018). Southern California coastal response to the 2015–2016 El Niño. *Journal of Geophysical Research: Earth Surface*, *123*(11), 3069–3083. https://doi.org/10.1029/2018JF004771

Zăinescu, F., Anthony, E., Vespremeanu-Stroe, A., Besset, M., & Tătui, F. (2023). Concerns about data linking delta land gain to human action. *Nature*, *614*(7947), E20–E25. https://doi.org/10.1038/s41586-022-05624-x